© 2015. Published by The Company of Biologists Ltd | Development (2015) 142, 314-319 doi:10.1242/dev.115998

RESEARCH REPORT

$VEGF_{189}$ binds NRP1 and is sufficient for VEGF/NRP1-dependent neuronal patterning in the developing brain

Miguel Tillo[1], Lynda Erskine[2], Anna Cariboni[1,3], Alessandro Fantin[1], Andy Joyce[1], Laura Denti[1] and Christiana Ruhrberg[1,*]

ABSTRACT

The vascular endothelial growth factor (VEGFA, VEGF) regulates neurovascular patterning. Alternative splicing of the *Vegfa* gene gives rise to three major isoforms termed $VEGF_{121}$, $VEGF_{165}$ and $VEGF_{189}$. $VEGF_{165}$ binds the transmembrane protein neuropilin 1 (NRP1) and promotes the migration, survival and axon guidance of subsets of neurons, whereas $VEGF_{121}$ cannot activate NRP1-dependent neuronal responses. By contrast, the role of $VEGF_{189}$ in NRP1-mediated signalling pathways has not yet been examined. Here, we have combined expression studies and *in situ* ligand-binding assays with the analysis of genetically altered mice and *in vitro* models to demonstrate that $VEGF_{189}$ can bind NRP1 and promote NRP1-dependent neuronal responses.

KEY WORDS: Vascular endothelial growth factor (VEGF), VEGF189, Neuron, Neuropilin, Mouse

INTRODUCTION

Vascular endothelial growth factor A (VEGFA, VEGF) is a potent inducer of blood vessel growth, but also has essential roles in neurodevelopment (Mackenzie and Ruhrberg, 2012). In humans, VEGF is encoded by a single gene (*VEGFA*) of eight exons that is alternatively spliced into isoforms, the major ones containing 121, 165 and 189 amino acid residues and therefore termed $VEGF_{121}$, $VEGF_{165}$ and $VEGF_{189}$, respectively (Fig. 1A; Koch et al., 2011). The alternatively spliced exons 6 and 7 encode domains that enable extracellular matrix (ECM) binding and additionally mediate differential binding to VEGF receptors. All VEGF isoforms bind the receptor tyrosine kinases VEGFR1 (FLT1) and VEGFR2 (KDR, FLK1), whereas the non-catalytic receptors neuropilin (NRP) 1 and NRP2 are VEGF isoform-specific receptors that preferentially bind $VEGF_{165}$ over $VEGF_{121}$ (Fig. 1A; Gluzman-Poltorak et al., 2000; Soker et al., 1998). Unexpectedly, recent studies showed that VEGF binding to NRP1 is largely dispensable for embryonic angiogenesis (Fantin et al., 2014). By contrast, VEGF signalling through NRP1 has multiple roles in neurodevelopment, including guiding migrating facial branchiomotor (FBM) neurons in the hindbrain (Schwarz et al., 2004), promoting the survival of migrating gonadotropin-releasing hormone (GnRH) neurons (Cariboni et al., 2011) and enhancing the contralateral projection of retinal ganglion cell (RGC) axons across the optic chiasm (Erskine et al., 2011).

To demonstrate roles for VEGF binding to NRP1 in neurons, prior studies used $Vegfa^{120/120}$ mice, which express $VEGF_{120}$, the murine equivalent of $VEGF_{121}$, but lack $VEGF_{164}$ and $VEGF_{188}$, corresponding to human $VEGF_{165}$ and $VEGF_{189}$, respectively (Carmeliet et al., 1999). $Vegfa^{120/120}$ mice phenocopy the defects of NRP1 knockouts in FBM neuron migration, GnRH neuron survival and RGC axon guidance (Cariboni et al., 2011; Erskine et al., 2011; Schwarz et al., 2004). In all three systems, VEGF signalling was attributed to the activity of $VEGF_{165}$ because it evokes appropriate neuronal responses in tissue culture models (Cariboni et al., 2011; Erskine et al., 2011; Schwarz et al., 2004), and because the ability of NRP1 to bind $VEGF_{165}$ is well established (Fantin et al., 2014; Soker et al., 1998). However, $Vegfa^{120/120}$ mutants lack $VEGF_{188}$ in addition to $VEGF_{164}$. Yet, it has never previously been examined whether $VEGF_{189}$ can also function as a NRP1 ligand *in vivo*. Moreover, it is not known whether $VEGF_{121}$ can bind NRP1 in a physiologically relevant context, even though it has been suggested that the exon 8 domain, which is present in all major VEGF isoforms, including $VEGF_{121}$, can mediate NRP1 binding *in vitro* (Jia et al., 2006; Pan et al., 2007; Parker et al., 2012).

Here, we have generated alkaline phosphatase (AP)-conjugated VEGF isoforms for *in situ* ligand-binding assays (Fantin et al., 2014) to examine whether $VEGF_{121}$ or $VEGF_{189}$ can bind NRP1 *in vivo*, as previously reported for $VEGF_{165}$. Our studies demonstrate that $VEGF_{189}$ binds NRP1-expressing axon tracts in intact hindbrain tissue, but that $VEGF_{121}$ is unable to do so. We further show that $VEGF_{188}$ is co-expressed with the other isoforms during VEGF/NRP1-dependent FBM migration, GnRH neuron survival and RGC axon guidance, and that $VEGF_{188}$ is sufficient to control all three processes, whereas $VEGF_{120}$ is not. We conclude that $VEGF_{188}$ effectively binds NRP1 and has the capacity to evoke NRP1-dependent signalling events, similar to $VEGF_{164}$. Considering that $VEGF_{189}$ has the highest affinity for ECM and therefore tissue retention amongst the VEGF isoforms, future research may therefore wish to consider the mechanistic contribution and therapeutic potential of this understudied VEGF isoform.

RESULTS AND DISCUSSION

$VEGF_{188}$ is co-expressed with $VEGF_{120}$ and $VEGF_{164}$ in developing hindbrain, nose and diencephalon, and binds axons in a NRP1-dependent fashion

Because prior studies implicated VEGF signalling through NRP1 in FBM neuron migration in the hindbrain, GnRH neuron survival in the nose and RGC axon guidance in the diencephalon (Cariboni et al., 2011; Erskine et al., 2011; Schwarz et al., 2004), we asked which *Vegfa* isoforms were expressed in these developmental contexts. For this experiment, we designed isoform-specific primers that can distinguish the *Vegfa120*, *Vegfa164* and *Vegfa188* mRNA

[1]UCL Institute of Ophthalmology, University College London, 11-43 Bath Street, London EC1V 9EL, UK. [2]School of Medical Sciences, Institute of Medical Sciences, University of Aberdeen, Aberdeen AB25 2ZD, UK. [3]University of Milan, Department of Pharmacological and Biomolecular Sciences, Via Balzaretti 9, Milan 20133, Italy.

*Author for correspondence (c.ruhrberg@ucl.ac.uk)

Received 1 August 2014; Accepted 26 November 2014

Development (2015) 142, 314-319 doi:10.1242/dev.115998

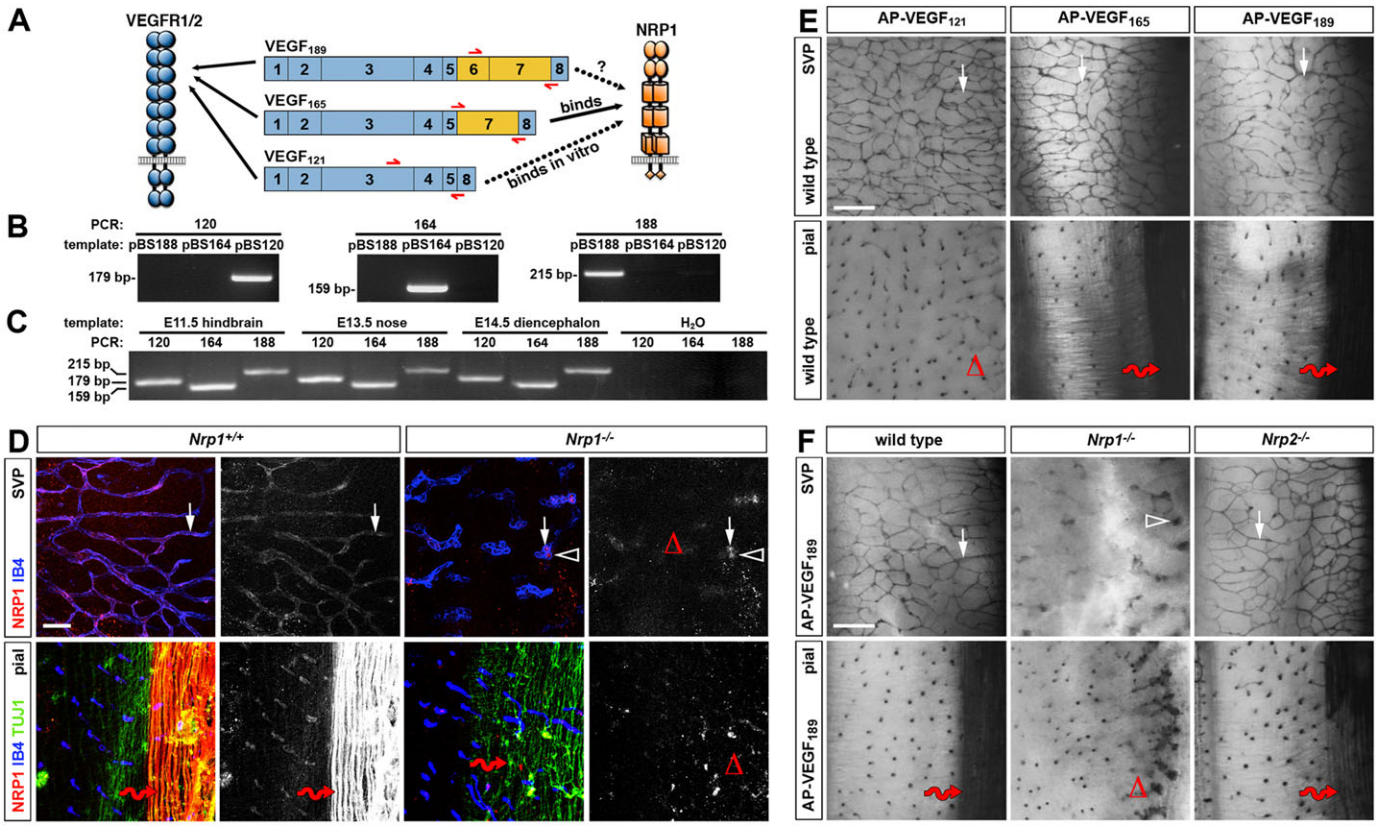

Fig. 1. $VEGF_{189}$ is expressed in developing mouse tissues and binds NRP1 in the developing hindbrain. (A) Current knowledge of VEGF isoform binding to their receptors. All isoforms bind VEGFR1/2, whereas only $VEGF_{165}$ is known to bind NRP1. $VEGF_{121}$ can bind NRP1 with low affinity *in vitro*, but whether this association occurs *in vivo* has not been shown. Moreover, it has not been shown whether $VEGF_{189}$ binds NRP1 *in vivo*. Red arrows below each isoform indicate the position of oligonucleotide primers used for RT-PCR in B. (B) *Vegfa* isoform-specific oligonucleotide primers for RT-PCR were validated with pBlueScript vectors (pBS) containing mouse *Vegfa120*, *Vegfa164* or *Vegfa188* cDNA, respectively. (C) RT-PCR analysis of the indicated tissues shows that *Vegfa120* (179 bp), *Vegfa164* (159 bp) and *Vegfa188* (215 bp) are co-expressed. (D) Whole-mount staining of E12.5 wild-type hindbrains for NRP1 and TUJ1 together with IB4; single NRP1 channels are shown in grey scale adjacent to each panel. The white arrows indicate IB4-positive vessels; the arrowhead indicates nonspecific NRP1 staining of blood cells inside mutant vessels; the red wavy arrows indicate TUJ1-positive axons; open triangles indicate absent NRP1 staining in subventricular plexus (SVP) vessels and pial axons. Scale bar: 200 µm. (E,F) AP-$VEGF_{121}$, AP-$VEGF_{165}$ and AP-$VEGF_{189}$ binding to E12.5 wild-type hindbrains (E) and AP-$VEGF_{189}$ binding to E12.5 *Nrp1*$^{-/-}$ and *Nrp2*$^{-/-}$ hindbrains (F). The white arrows indicate VEGF binding to vessels; the red wavy arrows indicate binding to axons; the open triangles indicate absence of $VEGF_{121}$ binding to wild-type axons in E and absence of $VEGF_{189}$ binding to axons in *Nrp1*$^{-/-}$ hindbrains in F. The arrowhead indicates vascular tufts. Scale bars: 25 µm.

species by reverse transcription (RT)-PCR (Fig. 1A,B; supplementary material Fig. S1A). This analysis demonstrated that all three isoforms were co-expressed during relevant periods of VEGF/NRP1-dependent neurodevelopment in mice (Fig. 1C).

Because prior studies of VEGF binding to NRP1 have not examined whether $VEGF_{189}$ or $VEGF_{121}$ can bind NRP1 *in vivo*, we used the mouse hindbrain as a physiologically relevant model to compare the ability of the three major VEGF isoforms to bind NRP1 in a tissue context. We first performed immunostaining with a validated antibody for NRP1 (Fantin et al., 2010) to confirm that NRP1 localises to blood vessels in wild-type, but not NRP1 knockout, hindbrains (Fig. 1D; note unspecific staining of blood in the dilated vessels of mutants). Immunolabelling also confirmed NRP1 expression in TUJ1-positive dorsolateral axons on the pial side of wild-type, but not mutant, hindbrains (Fig. 1D; supplementary material Fig. S1B). *Nrp1*$^{-/-}$ hindbrains showed some defasciculation of these dorsolateral axons, but they were still clearly present in the mutant, suggesting that this are a suitable model to examine VEGFA isoform binding to NRP1.

To compare the binding properties of $VEGF_{121}$, $VEGF_{165}$ and $VEGF_{189}$, we fused each isoform to AP and performed *in situ* ligand binding assays on E12.5 hindbrains. As expected, all three isoforms bound vessels (Fig. 1E), because they express the pan-VEGF isoform receptor VEGFR2 (Lanahan et al., 2013). We next examined binding to dorsolateral axons, because they express NRP1, but lack VEGFR2 (Lanahan et al., 2013). Both $VEGF_{165}$ and $VEGF_{189}$ bound these axons, whereas $VEGF_{121}$ did not (Fig. 1E). These observations indicate that all VEGF isoforms are capable of binding VEGFR2/NRP1-positive vessels. By contrast, only $VEGF_{165}$ and $VEGF_{189}$, but not $VEGF_{121}$, bound NRP1-expressing axons lacking VEGFR2, consistent with the previously reported 10-fold lower affinity of $VEGF_{121}$ for NRP1 *in vitro* (Parker et al., 2012). The finding that $VEGF_{121}$ does not bind endogenous neuronal NRP1 at detectable levels also agrees with prior genetic studies, which showed that $VEGF_{120}$ is unable to compensate for $VEGF_{164}$ in FBM, RGC and GnRH neurons (Cariboni et al., 2011; Erskine et al., 2011; Schwarz et al., 2004). Thus, low-affinity binding of $VEGF_{121}$ to NRP1, even though previously observed *in vitro*, is unlikely to be relevant *in vivo*, at least in a neuronal context.

We next confirmed that axonal $VEGF_{189}$ binding is NRP1 dependent. The AP ligand-binding assay showed that $VEGF_{189}$ bound vessels (Fig. 1F) in *Nrp1*-null mutant hindbrains with their characteristic vascular tufts (Fantin et al., 2013a). Strikingly, AP-$VEGF_{189}$ failed to bind axons in *Nrp1*-null hindbrains, similar to AP-$VEGF_{165}$ (Fig. 1F). $VEGF_{189}$ can therefore bind axons in a

Development (2015) 142, 314-319 doi:10.1242/dev.115998

NRP1-dependent fashion. By contrast, loss of NRP2 (Giger et al., 2000) did not abolish $VEGF_{189}$ binding (Fig. 1F). Taken together, the ligand binding assays of intact hindbrain tissue show that NRP1 serves as a neuronal receptor for $VEGF_{165}$ and $VEGF_{189}$, but not for $VEGF_{121}$.

$VEGF_{188}$ is sufficient for the NRP1-dependent migration of FBM neurons

Vegfa is a haploinsufficient gene for which deletion of just one allele results in early embryonic lethality due to a complete failure of blood vessel formation (Carmeliet et al., 1996; Ferrara et al., 1996). However, retention of any one of the major VEGF isoforms rescues this severe phenotype and instead gives rise to more subtle neuronal and vascular phenotypes (Ruhrberg et al., 2002; Stalmans et al., 2002). Understanding the receptor-binding properties of the VEGF isoforms has therefore become a priority in the field. We first examined if $VEGF_{188}$ can substitute for $VEGF_{164}$ in FBM neuron guidance with an established hindbrain explant assay in which implanted beads provide exogenous VEGF, and FBM neuron migration is visualised by immunolabelling with the motor neuron marker ISL1 (Schwarz et al., 2004; Tillo et al., 2014). Agreeing with previous observations, FBM neurons were attracted to $VEGF_{164}$, but not to control beads lacking growth factors (Fig. 2B). $VEGF_{188}$ beads also attracted FBM neurons (Fig. 2B). Quantification confirmed that FBM neuron migration was significantly enhanced on the hindbrain side containing a $VEGF_{164}$- or $VEGF_{188}$-soaked bead relative to the control side of the same hindbrain (Fig. 2C). $VEGF_{188}$ can therefore promote NRP1-dependent neuronal migration similar to $VEGF_{164}$.

We next examined FBM neuron migration *in vivo* by *Isl1 in situ* hybridisation. As previously shown (Schwarz et al., 2004), $Vegfa^{120/120}$ hindbrains demonstrated abnormal streaming of FBM neurons on the ventricular side and dumbbell-shaped nuclei on the pial side (Fig. 2D). By contrast, $Vegfa^{188/188}$ mice, which express only $VEGF_{188}$, showed normal FBM neuron migration (Fig. 2D). Moreover, replacing one $Vegfa^{120}$ allele in $Vegfa^{120/120}$ mutants with the $Vegfa^{188}$ allele was sufficient to prevent FBM neuron defects (Fig. 2D). Unlike $VEGF_{120}$, $VEGF_{188}$ is therefore sufficient to direct NRP1-dependent neuronal migration.

$VEGF_{188}$ is sufficient to guide NRP1-dependent axon crossing at the optic chiasm

We next investigated whether $VEGF_{188}$ can evoke neuronal responses similar to $VEGF_{164}$ in the developing visual system. To establish binocular vision, RGC axons project through the optic chiasm to both the ipsilateral and contralateral brain hemispheres (Erskine and Herrera, 2007). $VEGF_{164}$, but not $VEGF_{120}$, promotes RGC axon guidance in a NRP1-dependent fashion *in vitro*, and $Vegfa^{120/120}$ mice therefore develop an abnormal chiasm (Erskine et al., 2011). To examine whether $VEGF_{188}$ can also promote RGC axon guidance, we performed DiI labelling in VEGF isoform mutants. Anterograde labelling of RGC axons from one eye at E14.5 demonstrated that $VEGF_{188}$ was sufficient for NRP1-mediated chiasm patterning (Fig. 3A). Thus, $Vegfa^{120/120}$ mice had a significantly increased ipsilateral projection index as well as defasciculation of the ipsilateral and contralateral optic tracts (Erskine et al., 2011), but the ipsilateral index and shape of the optic chiasm appeared unaffected in $Vegfa^{188/188}$ mice (Fig. 3B,C). Moreover, replacing one $Vegfa^{120}$ with the $Vegfa^{188}$ allele was sufficient to prevent chiasm defects in $Vegfa^{120/120}$ mutants (Fig. 3B,C).

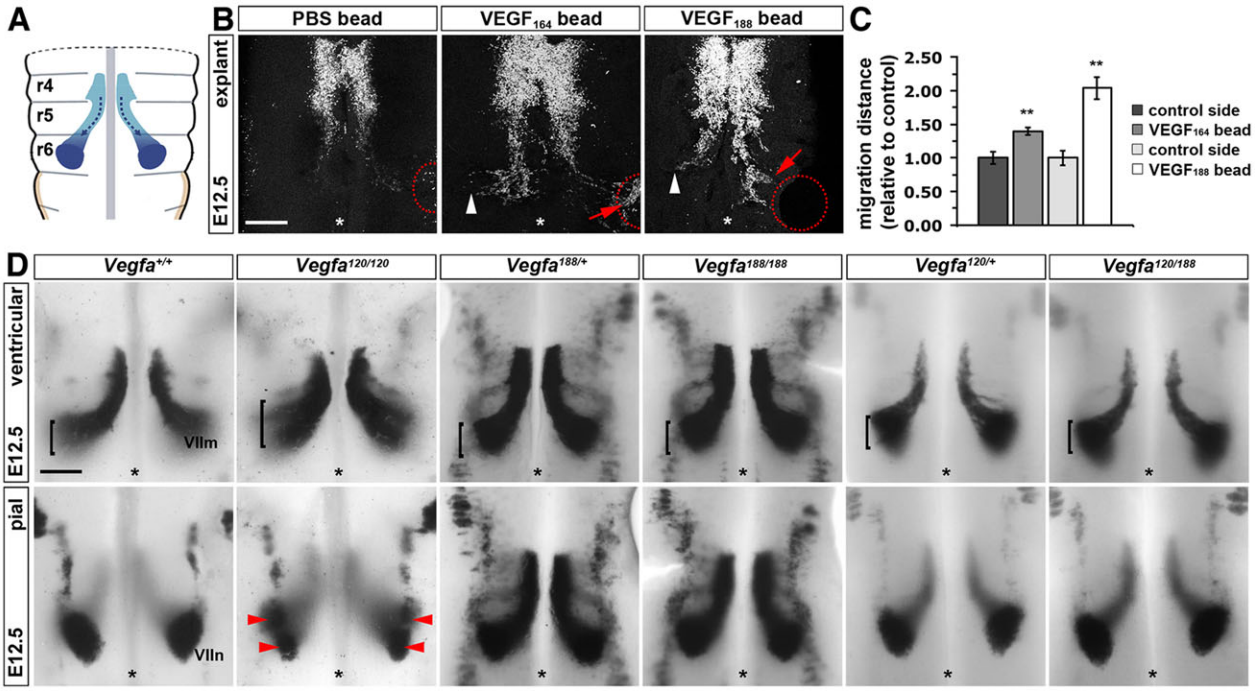

Fig. 2. $VEGF_{188}$ is sufficient for FBM neuron migration. (A) Schematic representation of FBM neuron migration in the mouse. (B) ISL1 staining of E12.5 hindbrain explants containing implanted heparin beads soaked in PBS (n=10) or PBS containing $VEGF_{164}$ (n=10) or $VEGF_{188}$ (n=6). Red dotted circles indicate the position of heparin beads; white arrowheads indicate normal migration; red arrows indicate migration towards heparin beads; asterisks indicate the midline. Scale bar: 200 µm. (C) Distance migrated by FBM neurons. Migration distance was quantified as migration away from r5 territory on the hindbrain side with a bead relative to the control half of the same hindbrain; mean±s.e.m. control 1±0.09 versus $VEGF_{164}$ bead 1.39±0.05; control 1±0.11 versus $VEGF_{188}$ bead 2.04±0.17; $^{**}P$<0.01, VEGF compared with control (t-test). (D) Whole-mount *Isl1 in situ* hybridisation of E12.5 hindbrains of the indicated genotypes detects migrating FBM neurons (VIIm) (control, n=10; $Vegfa^{120/120}$, n=6; $Vegfa^{188/188}$, n=4; $Vegfa^{120/188}$, n=5). Brackets indicate the width of the neuronal stream on the ventricular side; red arrowheads indicate dumbbell-shaped nuclei on the pial side; asterisks indicate the midline. Scale bar: 25 µm.

Development (2015) 142, 314-319 doi:10.1242/dev.115998

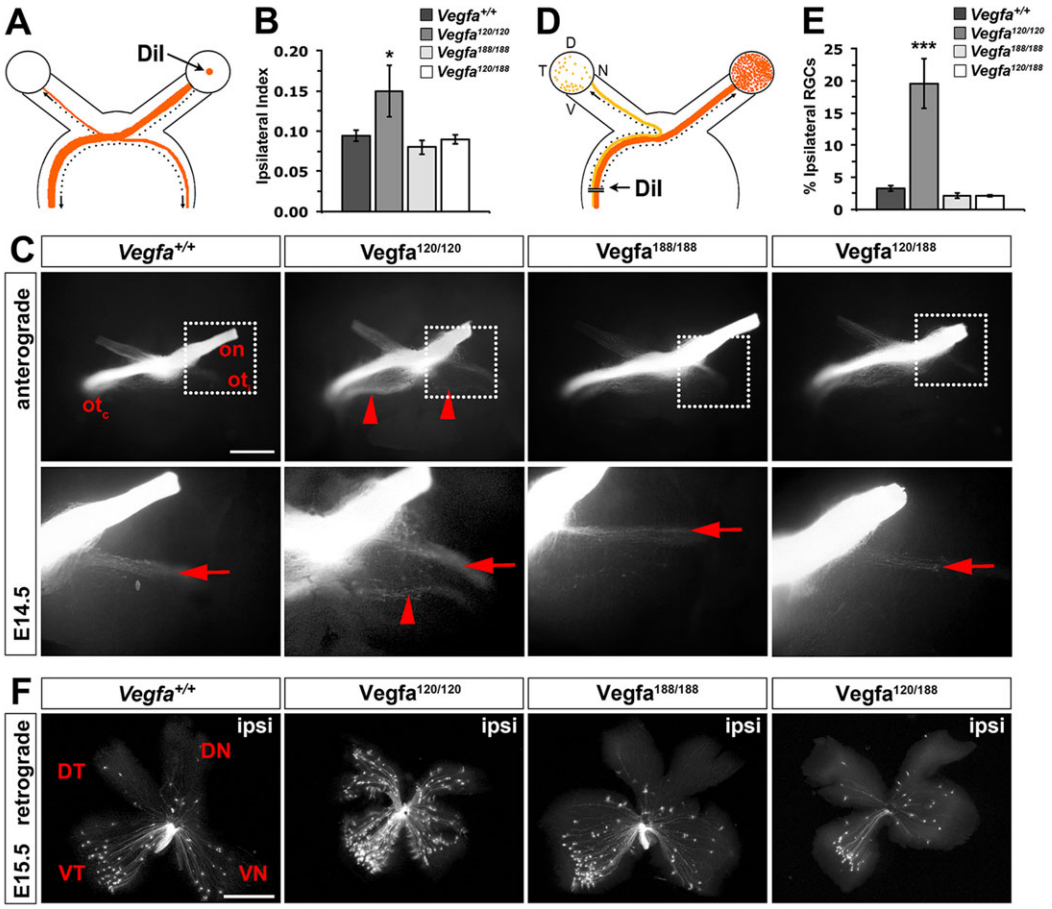

Fig. 3. VEGF$_{188}$ is sufficient to guide commissural axons across the optic chiasm. (A) Schematic illustration of the method used to anterogradely label RGC projections. DiI crystals were placed onto the retina in one eye to label axons extending through the optic chiasm into the ipsilateral and contralateral optic tracts. (B) Ipsilateral index in the indicated genotypes (mean±s.e.m.): control, 0.095±0.01, *n*=11; *Vegfa*$^{120/120}$, 0.15±0.03, *n*=5; *Vegfa*$^{188/188}$, 0.083±0.01, *n*=3; *Vegfa*$^{120/188}$, 0.09±0.01, *n*=3; *t*-test, **P*<0.05 compared with control. (C) Whole-mount views of RGC axons at the optic chiasm from embryos of the indicated genotypes, labelled anterogradely with DiI at E14.5; ventral view, anterior upwards; optic nerve (on), contralateral optic tract (ot$_c$) and ipsilateral optic tract (ot$_i$). Red arrows indicate the normal position of the ipsilateral projection; red arrowheads indicate the secondary tract and axon defasciculation in *Vegfa*$^{120/120}$ mutants. Scale bar: 500 µm. Higher magnifications of each boxed areas are shown beneath the respective panels. (D) Schematic illustration of the method used to retrogradely label RGC projections. DiI crystals were placed unilaterally into the optic tract in the dorsal thalamus. (E) Proportion of ipsilaterally projecting RGCs relative to total number of RGCs in both eyes of the indicated genotypes at E15.5 (mean±s.e.m.): control, 3.28±0.44%, *n*=8; *Vegfa*$^{120/120}$, 19.64±3.89%, *n*=4; *Vegfa*$^{188/188}$, 2.16±0.42%, *n*=4; *Vegfa*$^{120/188}$, 2.12±0.14%, *n*=2; *t*-test, ****P*<0.001 compared with control. (F) Flatmounted ipsilateral retinas from E15.5 embryos of the indicated genotypes after retrograde labelling from the optic tract in the right thalamus. DT, dorsotemporal; VN, ventronasal; DN, dorsonasal; VT, ventrotemporal. Scale bar: 500 µm.

We next performed retrograde DiI labelling of RGC axons from the dorsal thalamus in VEGF isoform mice and compared the number of labelled RGCs in flatmounted ipsilateral and contralateral retina (Fig. 3D). Quantitation showed that the proportion of DiI-labelled ipsilateral RGCs was significantly increased in *Vegfa*$^{120/120}$ compared with control mice, but was normal in *Vegfa*$^{188/188}$ and *Vegfa*$^{120/188}$ mice (Fig. 3E). Flat-mount images also revealed the preferential origin of ipsilaterally projecting neurons from the ventrotemporal retina in wild types (Fig. 3F). Their distribution is affected in *Vegfa*$^{120/120}$ mice, which contain ipsilaterally projecting RGCs throughout the nasal retina (Erskine et al., 2011), but this defect was rescued by the introduction of a single *Vegfa*^{188} allele (Fig. 3F). VEGF$_{188}$ is therefore sufficient to promote NRP1-dependent aspects of optic chiasm development.

VEGF$_{188}$ is sufficient to ensure normal GnRH neuron survival

As a third model to study VEGF$_{188}$ in neurodevelopment, we investigated GnRH neuron survival. GnRH neurons are born in the nasal placode and travel along nasal axons to reach the forebrain (Fig. 4A; Cariboni et al., 2007). We have previously shown that *Vegfa*$^{120/120}$ mice have significantly fewer migrating GnRH neurons and demonstrated that VEGF$_{164}$ signals through NRP1 to promote the survival of GN11 cells, which recapitulate many features of migratory GnRH neurons (Cariboni et al., 2011). We therefore examined whether VEGF$_{188}$ promotes GN11 survival, similar to VEGF$_{164}$. Whereas 72 h of serum withdrawal caused the death of over half of the GN11 cells, the inclusion of serum, VEGF$_{164}$ or VEGF$_{188}$ for the last 12 h of culture significantly reduced cell death, and VEGF$_{188}$ was as effective as VEGF$_{164}$ in preventing cell death; by contrast, and as expected, VEGF$_{120}$ did not promote survival (Fig. 4B; percentage of propidium iodide-positive cells, mean±s.e.m.: control, 44±3%; serum, 2±1%; VEGF$_{120}$, 37±3; VEGF$_{164}$, 11±2%; VEGF$_{188}$, 11±2%). These observations suggest that VEGF$_{188}$, similar to VEGF$_{164}$, can promote GnRH neuron survival. The ineffectiveness of VEGF$_{120}$ agreed with the previously observed NRP1-dependent neuroprotection of GN11 cells and the

Development (2015) 142, 314-319 doi:10.1242/dev.115998

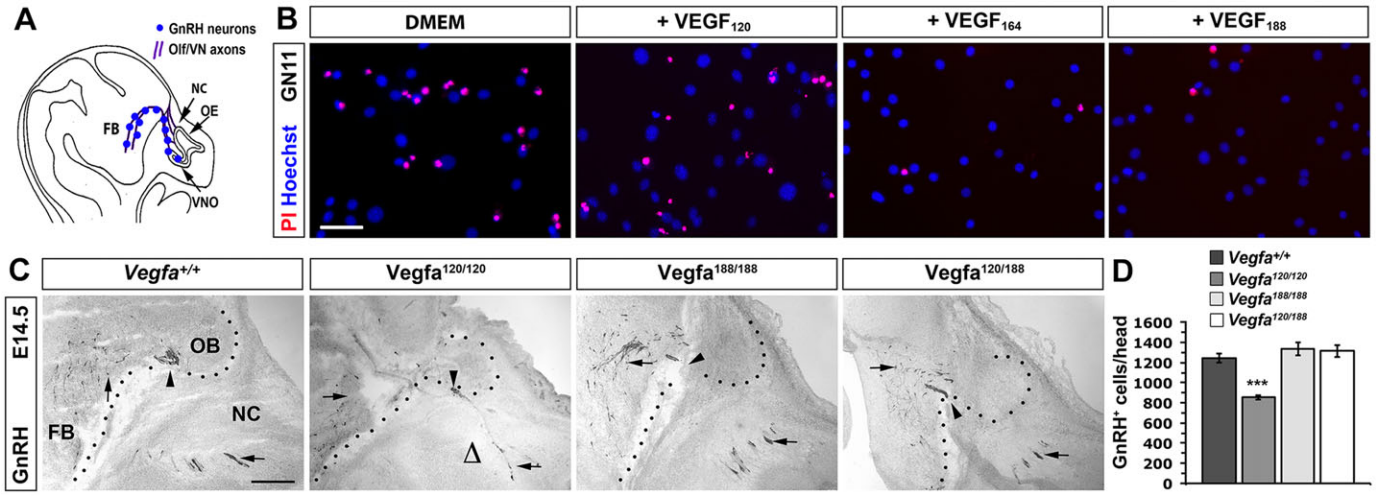

Fig. 4. $VEGF_{188}$ is sufficient to promote GnRH neuron survival. (A) GnRH neuron migration (blue dots). The neurons are born in the nasal placodes that give rise to the olfactory and vomeronasal epithelia (OE, VNO) and migrate along olfactory and vomeronasal axons (purple, Olf/VN) through the nasal compartment (NC) to reach the forebrain (FB). (B) Serum-starved GN11 cells were treated with DMEM or DMEM-containing serum, $VEGF_{120}$, $VEGF_{164}$ or $VEGF_{188}$; cell death was visualised by propidium iodide staining (red); Hoechst staining (blue) identified the total number of cells. Scale bar: 25 µm. (C) Sagittal sections of E14.5 mouse heads of the indicated genotypes, immunolabelled for GnRH. Arrows indicate migrating neurons; arrowheads indicate blood vessels; open triangles indicate the absence of migrating neurons; dotted lines indicate the FB boundary. OB, olfactory bulb. Scale bar: 100 µm. (D) GnRH neuron number in E14.5 heads of the indicated genotypes (mean±s.e.m.): control, 1246±46, *n*=6; *Vegfa*$^{120/120}$, 854±21, *n*=5; *Vegfa*$^{188/188}$, 1335±63, *n*=3; *Vegfa*$^{120/188}$, 1314±58, *n*=3; *t*-test; ***P<0.001 compared with control.

fact that *Vegfa*$^{120/120}$ mice have fewer GnRH neurons (Cariboni et al., 2011). Also in agreement with the *in vitro* findings, the GnRH neuron number was normal in *Vegfa*$^{188/188}$ mice that express $VEGF_{188}$ but lack $VEGF_{164}$ (Fig. 4C,D). Moreover, replacing one *Vegfa*^{120} allele in *Vegfa*$^{120/120}$ mutants with the *Vegfa*^{188} allele was sufficient to prevent their GnRH neuron survival defect (Fig. 4C,D). Together, these data show that $VEGF_{188}$ is sufficient to promote NRP1-dependent neuronal survival.

Conclusions

Our study has demonstrated that human $VEGF_{189}$, but not $VEGF_{121}$, binds NRP1 in a tissue context, that mouse $VEGF_{188}$ is co-expressed with $VEGF_{164}$ in a neuronal context, and that mouse $VEGF_{188}$ expressed from the endogenous *Vegfa* locus can evoke NRP1-dependent neuronal responses *in vitro* and *in vivo*, similar to $VEGF_{164}$ and unlike $VEGF_{121}$. Future work on the role of VEGF signalling through NRP1, especially studies using *Vegfa*$^{120/120}$ or tissue-specific *Vegfa*-null alleles, should therefore consider the possibility that $VEGF_{188}$, similar to $VEGF_{164}$, can regulate the process under investigation. This consideration would be relevant for both neural and vascular studies, or indeed any context in which VEGF signalling through NRP1 is implicated. The finding that the relatively understudied $VEGF_{189}$ is capable of evoking VEGF isoform-specific signalling events may have broad implications for the therapeutic use of VEGF. Thus, VEGF application has been considered in many studies for pro-angiogenic, pro-neurogenic and neuroprotective therapies, e.g. the treatment of amyotrophic lateral sclerosis (reviewed by Storkebaum et al., 2011). Most prior studies have used $VEGF_{165}$ to ensure comprehensive receptor targeting; however, the retention of $VEGF_{165}$ in tissues is inferior to that of $VEGF_{189}$ due to the presence of only one instead of two heparin/matrix-binding domains. Our work demonstrating that $VEGF_{189}$ is fully capable of engaging NRP1, in addition to its known ability to bind VEGFR1 and VEGFR2, therefore suggests that $VEGF_{189}$ may be better suited than $VEGF_{165}$ to induce localised tissue effects in therapeutic applications.

MATERIALS AND METHODS

Animals

Animal procedures were preformed in accordance with institutional and UK Home Office guidelines. The *Vegfa*^{120} and *Vegfa*^{188} alleles (Carmeliet et al., 1999; Stalmans et al., 2002), and *Nrp1*$^{-/-}$ and *Nrp2*$^{-/-}$ mice have been described previously (Giger et al., 2000; Kitsukawa et al., 1997).

RT-PCR and sequencing

Total RNA was reverse transcribed using Superscript III (Life Technologies) and *Vegfa* isoforms amplified by PCR using MegaMix (Microzone) and the following oligonucleotide pairs: 120-F 5′-GTAACGATGAAGCCCTG-GAG-3′ and 120-R 5′-CCTTGGCTTGTCACATTTTTC-3′; 164-F 5′-AG-CCAGAAAATCACTGTGAGC-3′ and 164-R 5′-GCCTTGGCTTGTCA-CATCT-3′; 188-F 5′-AGTTCGAGGAAAGGGAAAGG-3′ and 188-R 5′-GCCTTGGCTTGTCACATCT-3′.

AP-fusion protein binding assays

Open reading frames for the VEGF isoforms were amplified by PCR with the oligonucleotides 5′-AATAATGGATCCGCACCCATGGCAGAAGG-AG-3′ and 5′-TATATGCTCGAGCTCACCGCCTCGGCTTGTC-3′. The PCR products were cloned into pAG3-AP containing an upstream in-frame AP cassette. Binding assay were performed as described previously (Fantin et al., 2013b).

Immunolabelling and *in situ* hybridisation

Primary antibodies used were: rabbit anti-mouse GnRH (Immunostar, 20075, 1:1000), goat anti-rat NRP1 (R&D Systems, AF566, 1:100), rabbit anti-mouse TUJ1 (Covance, MRB-435p, 1:250) and mouse anti-rat ISL1 (DSHB, 39.4D5, 1:100). Secondary antibodies used were: Alexa594-conjugated rabbit anti-goat Fab (Jackson ImmunoResearch, 305-587-003, 1:200), Alexa488-conjugated donkey anti-rabbit Fab (Jackson ImmunoResearch, 711-547-003, 1:200), Alexa488-conjugated goat anti-mouse (Life Technologies, A-110011, 1:200) and biotinylated goat anti-rabbit (Vector Laboratories, BA-1000, 1:200). To detect blood vessels, we used biotinylated IB4 (Sigma) followed by Alexa633-conjugated streptavidin (Life Technologies). For *in situ* hybridisation, we used a digoxigenin-labelled *Isl1* probe (Schwarz et al., 2004).

Development (2015) 142, 314-319 doi:10.1242/dev.115998

Hindbrain explant culture

Hindbrain explants were cultured as previously described (Schwarz et al., 2004; Tillo et al., 2014). Affi-Gel heparin beads (Bio-Rad) were soaked overnight in 100 ng/ml of $VEGF_{164}$ in PBS (Preprotech) or $VEGF_{188}$ (Reliatech). FBM neuron migration was measured with ImageJ (NIH) as the distance travelled from r5 to the leading group of cells in r6 in each hindbrain and normalised to the control side of each hindbrain.

DiI labelling

DiI labelling was performed with fixed tissues as described previously (Erskine et al., 2011). Briefly, a DiI crystal (Life Technologies) was placed over the optic disc of one eye for anterograde labelling. After 3 days at 37°C, dissected brains were imaged ventral side upwards. ImageJ was used to determine the pixel intensity in defined areas of the ipsilateral and contralateral optic tracts, and the ipsilateral index calculated as the ratio of fluorescent intensity in the ipsilateral relative to the ipsilateral plus contralateral tracts. For retrograde labelling, the cortex was removed unilaterally and DiI crystals placed in a row over the dorsal thalamus for 15 weeks at room temperature; we imaged flatmounted retinas as above and determined the percentage of labelled ipsilateral RGCs relative to the ipsilateral plus contralateral RGCs.

GnRH neuron analysis and survival assays

Immunolabelled GnRH-positive cells were quantitated and GN11 survival assays performed as described previously (Cariboni et al., 2011). For survival assays, cells were serum starved for 72 h and treated for 12 h with media containing 10% FBS, 10 ng/ml $VEGF_{120}$, $VEGF_{164}$ or $VEGF_{188}$.

Acknowledgements

We thank Dr Jonathan Raper for the pAG3-AP plasmid and the staff of the Biological Resources Unit at the UCL Institute of Ophthalmology for help with mouse husbandry.

Competing interests

The authors declare no competing financial interests.

Author contributions

C.R. and M.T. planned the experiments and wrote the manuscript. M.T., L.E., A.C., A.F., A.J., L.D. and C.R. performed the experiments. All authors have read, commented on and approved the manuscript.

Funding

This research was funded by a Wellcome Trust PhD fellowship to M.T. [092839/Z/10/Z] and a BBSRC project grant to C.R. and L.E. [BB/J00930X/1]. Deposited in PMC for immediate release.

Supplementary material

Supplementary material available online at
http://dev.biologists.org/lookup/suppl/doi:10.1242/dev.115998/-/DC1

References

Cariboni, A., Maggi, R. and Parnavelas, J. G. (2007). From nose to fertility: the long migratory journey of gonadotropin-releasing hormone neurons. *Trends Neurosci.* **30**, 638-644.

Cariboni, A., Davidson, K., Dozio, E., Memi, F., Schwarz, Q., Stossi, F., Parnavelas, J. G. and Ruhrberg, C. (2011). VEGF signalling controls GnRH neuron survival via NRP1 independently of KDR and blood vessels. *Development* **138**, 3723-3733.

Carmeliet, P., Ferreira, V., Breier, G., Pollefeyt, S., Kieckens, L., Gertsenstein, M., Fahrig, M., Vandenhoeck, A., Harpal, K., Eberhardt, C. et al. (1996). Abnormal blood vessel development and lethality in embryos lacking a single VEGF allele. *Nature* **380**, 435-439.

Carmeliet, P., Ng, Y.-S., Nuyens, D., Theilmeier, G., Brusselmans, K., Cornelissen, I., Ehler, E., Kakkar, V. V., Stalmans, I., Mattot, V. et al. (1999). Impaired myocardial angiogenesis and ischemic cardiomyopathy in mice lacking the vascular endothelial growth factor isoforms VEGF164 and VEGF188. *Nat. Med.* **5**, 495-502.

Erskine, L. and Herrera, E. (2007). The retinal ganglion cell axon's journey: insights into molecular mechanisms of axon guidance. *Dev. Biol.* **308**, 1-14.

Erskine, L., Reijntjes, S., Pratt, T., Denti, L., Schwarz, Q., Vieira, J. M., Alakakone, B., Shewan, D. and Ruhrberg, C. (2011). VEGF signaling through neuropilin 1 guides commissural axon crossing at the optic chiasm. *Neuron* **70**, 951-965.

Fantin, A., Vieira, J. M., Gestri, G., Denti, L., Schwarz, Q., Prykhozhij, S., Peri, F., Wilson, S. W. and Ruhrberg, C. (2010). Tissue macrophages act as cellular chaperones for vascular anastomosis downstream of VEGF-mediated endothelial tip cell induction. *Blood* **116**, 829-840.

Fantin, A., Vieira, J. M., Plein, A., Denti, L., Fruttiger, M., Pollard, J. W. and Ruhrberg, C. (2013a). NRP1 acts cell autonomously in endothelium to promote tip cell function during sprouting angiogenesis. *Blood* **121**, 2352-2362.

Fantin, A., Vieira, J. M., Plein, A., Maden, C. H. and Ruhrberg, C. (2013b). The embryonic mouse hindbrain as a qualitative and quantitative model for studying the molecular and cellular mechanisms of angiogenesis. *Nat. Protoc.* **8**, 418-429.

Fantin, A., Herzog, B., Mahmoud, M., Yamaji, M., Plein, A., Denti, L., Ruhrberg, C. and Zachary, I. (2014). Neuropilin 1 (NRP1) hypomorphism combined with defective VEGF-A binding reveals novel roles for NRP1 in developmental and pathological angiogenesis. *Development* **141**, 556-562.

Ferrara, N., Carver-Moore, K., Chen, H., Dowd, M., Lu, L., O'Shea, K. S., Powell-Braxton, L., Hillan, K. J. and Moore, M. W. (1996). Heterozygous embryonic lethality induced by targeted inactivation of the VEGF gene. *Nature* **380**, 439-442.

Giger, R. J., Cloutier, J.-F., Sahay, A., Prinjha, R. K., Levengood, D. V., Moore, S. E., Pickering, S., Simmons, D., Rastan, S., Walsh, F. S. et al. (2000). Neuropilin-2 is required in vivo for selective axon guidance responses to secreted semaphorins. *Neuron* **25**, 29-41.

Gluzman-Poltorak, Z., Cohen, T., Herzog, Y. and Neufeld, G. (2000). Neuropilin-2 is a receptor for the vascular endothelial growth factor (VEGF) forms VEGF-145 and VEGF-165. *J. Biol. Chem.* **275**, 18040-18045.

Jia, H., Bagherzadeh, A., Hartzoulakis, B., Jarvis, A., Lohr, M., Shaikh, S., Aqil, R., Cheng, L., Tickner, M., Esposito, D. et al. (2006). Characterization of a bicyclic peptide neuropilin-1 (NP-1) antagonist (EG3287) reveals importance of vascular endothelial growth factor exon 8 for NP-1 binding and role of NP-1 in KDR signaling. *J. Biol. Chem.* **281**, 13493-13502.

Kitsukawa, T., Shimizu, M., Sanbo, M., Hirata, T., Taniguchi, M., Bekku, Y., Yagi, T. and Fujisawa, H. (1997). Neuropilin-semaphorin III/D-mediated chemorepulsive signals play a crucial role in peripheral nerve projection in mice. *Neuron* **19**, 995-1005.

Koch, S., Tugues, S., Li, X., Gualandi, L. and Claesson-Welsh, L. (2011). Signal transduction by vascular endothelial growth factor receptors. *Biochem. J.* **437**, 169-183.

Lanahan, A., Zhang, X., Fantin, A., Zhuang, Z., Rivera-Molina, F., Speichinger, K., Prahst, C., Zhang, J., Wang, Y., Davis, G. et al. (2013). The neuropilin 1 cytoplasmic domain is required for VEGF-A-dependent arteriogenesis. *Dev. Cell* **25**, 156-168.

Mackenzie, F. and Ruhrberg, C. (2012). Diverse roles for VEGF-A in the nervous system. *Development* **139**, 1371-1380.

Pan, Q., Chathery, Y., Wu, Y., Rathore, N., Tong, R. K., Peale, F., Bagri, A., Tessier-Lavigne, M., Koch, A. W. and Watts, R. J. (2007). Neuropilin-1 binds to VEGF121 and regulates endothelial cell migration and sprouting. *J. Biol. Chem.* **282**, 24049-24056.

Parker, M. W., Xu, P., Li, X. and Vander Kooi, C. W. (2012). Structural basis for selective vascular endothelial growth factor-A (VEGF-A) binding to neuropilin-1. *J. Biol. Chem.* **287**, 11082-11089.

Ruhrberg, C., Gerhardt, H., Golding, M., Watson, R., Ioannidou, S., Fujisawa, H., Betsholtz, C. and Shima, D. T. (2002). Spatially restricted patterning cues provided by heparin-binding VEGF-A control blood vessel branching morphogenesis. *Genes Dev.* **16**, 2684-2698.

Schwarz, Q., Gu, C., Fujisawa, H., Sabelko, K., Gertsenstein, M., Nagy, A., Taniguchi, M., Kolodkin, A. L., Ginty, D. D., Shima, D. T. et al. (2004). Vascular endothelial growth factor controls neuronal migration and cooperates with Sema3A to pattern distinct compartments of the facial nerve. *Genes Dev.* **18**, 2822-2834.

Soker, S., Takashima, S., Miao, H. Q., Neufeld, G. and Klagsbrun, M. (1998). Neuropilin-1 is expressed by endothelial and tumor cells as an isoform-specific receptor for vascular endothelial growth factor. *Cell* **92**, 735-745.

Stalmans, I., Ng, Y.-S., Rohan, R., Fruttiger, M., Bouché, A., Yuce, A., Fujisawa, H., Hermans, B., Shani, M., Jansen, S. et al. (2002). Arteriolar and venular patterning in retinas of mice selectively expressing VEGF isoforms. *J. Clin. Invest.* **109**, 327-336.

Storkebaum, E., Quaegebeur, A., Vikkula, M. and Carmeliet, P. (2011). Cerebrovascular disorders: molecular insights and therapeutic opportunities. *Nat. Neurosci.* **14**, 1390-1397.

Tillo, M., Schwarz, Q. and Ruhrberg, C. (2014). Mouse hindbrain ex vivo culture to study facial branchiomotor neuron migration. *J. Vis. Exp.* **85**, e51397.

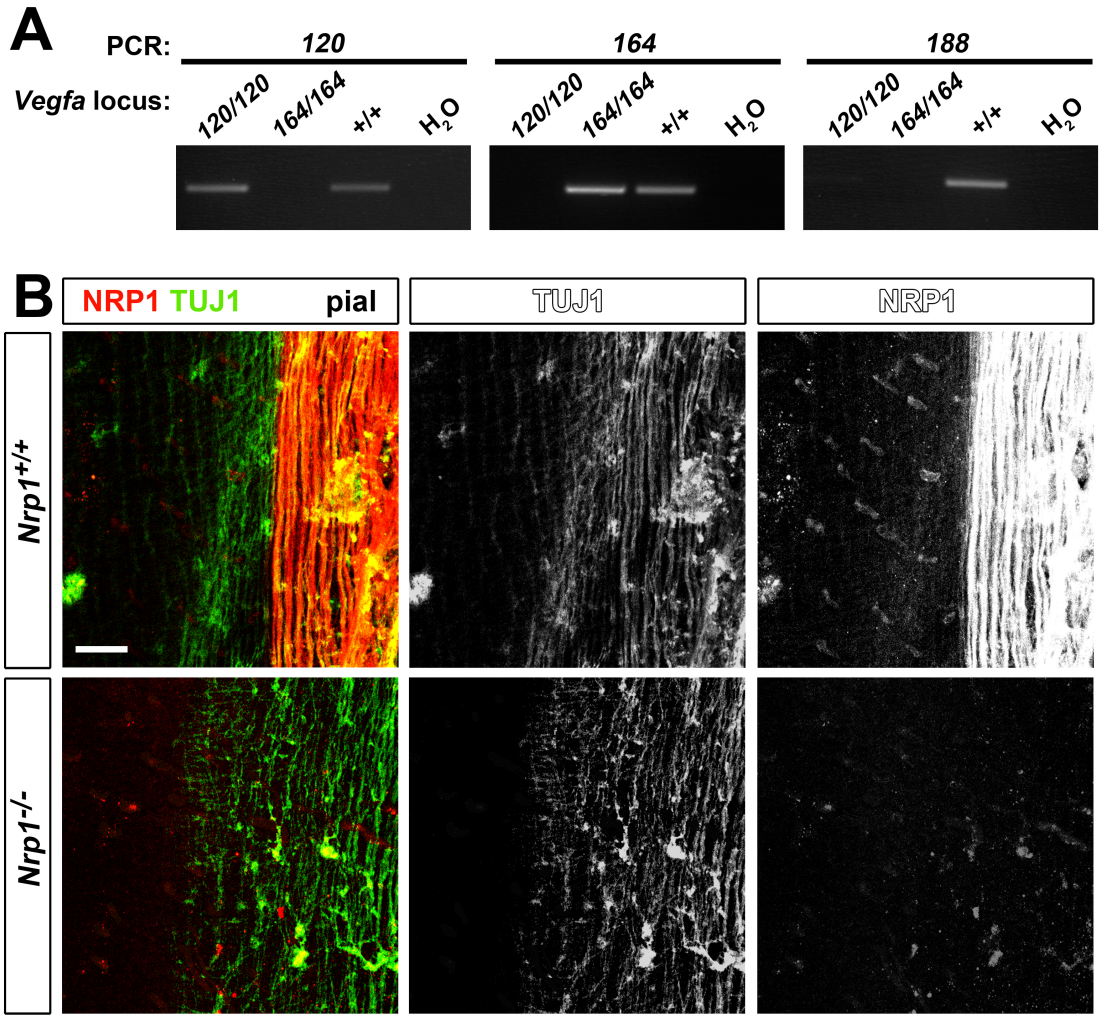

Fig. S1. ***Specificity of Vegfa isoform PCR reagents and perseverance of the dorsolateral fascicles in Nrp1-null mutants.***

(A) The specificity of oligonucleotide primers for *Vegfa* isoform expression analysis was validated by RT-PCR using cDNA derived from *Vegfa*$^{120/120}$, *Vegfa*$^{164/164}$ or wildtype E12.5 mouse embryo trunks, respectively. Note that a molecular weight standard confirmed the predicted sizes of each isoform as 179, 159 and 215 bp, respectively.

(**B**) Wholemount staining of E12.5 wildtype hindbrains for NRP1 and TUJ1; the single NRP1 and TUJ1 channels are shown in grey scale adjacent to each panel. Scale bar: 200 μm.